PLASMA DYNAMICS

X. PLASMA PHYSICS*

Academic and Research Staff

Prof. G. Bekefi	Prof. B. L. Wright	J. J. McCarthy
Prof. S. C. Brown	Dr. W. M. Manheimer	W. J. Mulligan
Prof. J. C. Ingraham		B. Rama Rao (Visiting Scientist)

Graduate Students

R. J. Becker	L. D. Pleasance	E. N. Spithas
A. J. Cohen	G. L. Rogoff	D. W. Swain
D. L. Flannery	J. K. Silk	J. H. Vellenga
L. P. Mix, Jr.		D. L. Workman

A. NONLINEAR COUPLING OF LOW-FREQUENCY OSCILLATIONS IN AN ELECTRON-CYCLOTRON RESONANCE DISCHARGE

We have previously described[1] the observation of spontaneously occurring low-frequency oscillations in an electron-cyclotron resonance microwave discharge. Here we report further measurements on these oscillations which indicate nonlinear coupling between the different low-frequency modes occurring in the plasma.

The geometry of the microwave waveguide, discharge tube, and magnetic field has been described in the previous report.[1] All experiments to be reported here were performed in helium gas at 0.02 Torr pressure. The discharge tube, as before, had an inner diameter of 1.3 cm.

We found it possible to seal off a tube containing 0.02 Torr helium with no subsequent deterioration of operating characteristics over a four-month period, provided the tube was initially baked at 400°C and the tube also contained an activated barium getter. The getter does not react with noble gas atoms, and hence provides a means of removing impurity gas atoms while not affecting the fill gas.

The oscillations were detected by measuring the low-frequency modulation of the microwave power reflected from the discharge, by capacitive pickup probes outside the discharge, and by electrical probes inserted into the discharge.

The low-frequency oscillation signal was fed into a 5-kHz to 5-MHz spectrum analyzer. Since a continuous recording of the oscillation frequencies and their amplitudes as a function of the magnetic field applied to the discharge was desired, a voltage output from the analyzer proportional to the oscillation amplitudes was used to modulate the beam intensity of a Tektronix oscilloscope. The horizontal sweep of the oscilloscope was triggered repetitively in synchronism with the analyzer sweep. The vertical deflection of the oscilloscope was driven by a voltage proportional to the magnetic field. Thus, as

*This work was supported principally by the U.S. Atomic Energy Commission (Contract AT(30-1)-1842).

the magnetic field was automatically scanned over the 4% (approximately) range for which a plasma could be produced, the oscilloscope beam traced out the evolution of the low-frequency oscillation spectrum of the plasma. The beam history was recorded by a time exposure photograph of the oscilloscope trace.

Figure X-1 shows data taken for a microwave frequency of 5.64 GHz and power of 0.4 Watt. The range of data on the vertical axis corresponds to a change of magnetic field from approximately 1975 Gauss to 2050 Gauss. For these operating conditions the oscillation frequencies are well defined, as can be seen from the figure. Also, generally more than one mode of oscillation is present. As the power is increased up to 1.2 Watts,

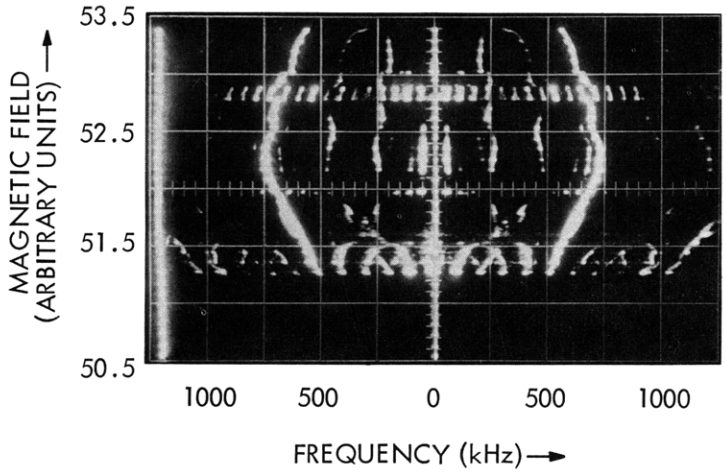

Fig. X-1. Low-frequency oscillation of the plasma. Microwave frequency, 5.64 GHz. Power, 0.4 W.

the maximum of the microwave generator, the low-frequency spectrum becomes partially obscured by background noise, but the pattern of behavior of the modes is the same as shown in Fig. X-1. As the power is reduced to 0.1 Watt, where the discharge is near extinguishing, the mode spectrum remains well-defined, but the lower frequency modes (<100 kHz) gradually disappear until at 0.1 Watt only the strong mode existing between 500 kHz and 750 kHz is easily detectable.

The nonlinear interaction between the modes is apparent in Fig. X-1 and in the data taken for the other conditions. Beginning at the top of the figure (magnetic field units ≈53.5), two dominant modes appear, one at ~600 kHz ("x") and the other near 200 kHz ("y"). By tracking the behavior of the third weaker oscillation that appears as the magnetic field is decreased, it is apparent that its frequency is given by x-y. As the magnetic field is decreased below 53.0 (arbitrary units) what appears to be a third mode, z, appears, having a fundamental frequency of 60 kHz and interacting strongly with

the x mode. The z mode disappears suddenly with a further decrease in magnetic field to 52.75. The x, y, and x-y oscillations evolve normally as the magnetic field is decreased to 52.0, with a slight hint of an oscillation of frequency x-2y, between 52.5 and 52.0, along with a mode resembling the z mode at 60 kHz. The behavior of all but the x mode is difficult to follow for magnetic fields lower than 52.0.

Further measurements are necessary to identify the waves associated with the x, y, and z modes. As pointed out in the previous report,[1] the order of magnitude of their frequencies can be correlated, respectively, with standing modes in the plasma of the ion cyclotron wave propagating nearly at 90° to the magnetic field, the electron drift wave, and the ion acoustic wave propagating parallel to the magnetic field.

Preliminary experiments in neon gas at 0.005 Torr pressure have revealed no oscillations. The present magnetic field homogeneity is uniform to ±1.5% over the active discharge region. It is felt that this should be improved before more interpretation of the data is attempted.

Interpretation is complicated by the fact that the same microwave signal that produces the plasma is also coupling energy into the low-frequency oscillations. In this connection, the question arises about whether the existence of these low-frequency oscillations depends on the fact that the microwave signal is also producing the plasma. That is, might these oscillations be analogous to the striations

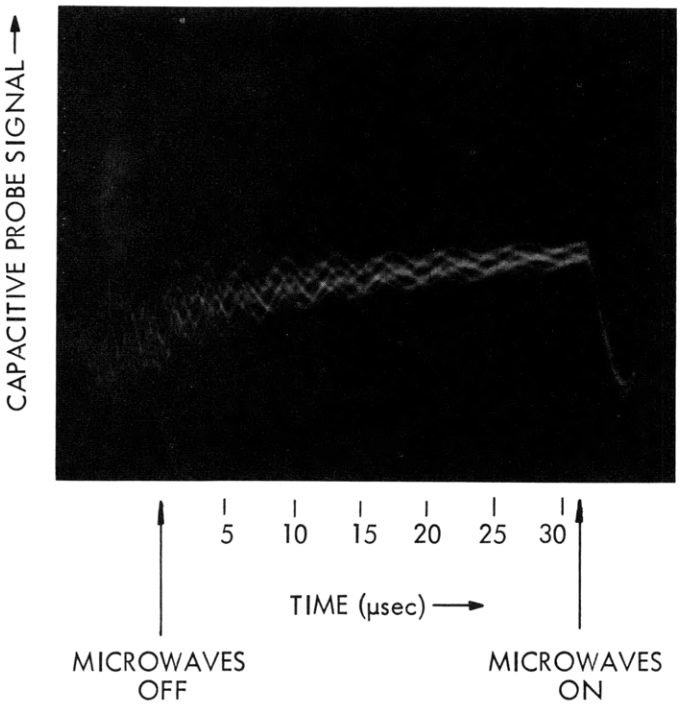

Fig. IX-2. High-frequency mode (x).

found in low-pressure DC discharges?

To test this hypothesis, the microwave signal was pulsed off for a period of 30 μsec, and then pulsed on again. This was done repetitively, and the oscillatory behavior of the plasma was monitored by displaying the output of probes capacitively coupled to the plasma on an oscilloscope trace. As is shown in Fig. X-2, the high-frequency mode (x) exists for at least 30 μsec after the microwave signal is terminated. Since the microwave signal is terminated in less than 1 μsec, there is an indication that the x mode is associated with a legitimate plasma wave. It is also apparent that the wave frequency decreases with time, thereby indicating a possible dependence on the electron temperature or density.

J. C. Ingraham

References

1. J. C. Ingraham and A. Novenski, Quarterly Progress Report No. 82, Research Laboratory of Electronics, M.I.T., July 15, 1966, p. 123.

B. NONLINEAR COUPLING OF LOW-FREQUENCY IONIZATION WAVES

1. Introduction

The object of this experiment is to study the nonlinear effects in low-amplitude ionization waves. These waves are similar to striations, the difference being that striations are usually thought of as very large amplitude waves, with highly nonsinusoidal waveforms. Low-amplitude waves can be generated in some cases with sinusoidal waveforms and voltage amplitudes that are much smaller than the electron temperature. As the amplitude of these waves is increased, nonlinear effects begin to become appreciable, and the characteristic flattened striation waveform is reached at high enough amplitudes.

Experimentally, the most easily seen effect of a small nonlinearity in the response of the plasma to a sinusoidal driving frequency is the generation of a signal at twice the frequency. If two waves of frequencies f_1 and f_2 are excited, then there will also be signals at $2f_1$, $2f_2$, and $f_1 \pm f_2$. The amplitudes of the sum and difference frequency signals should be proportional to the product of the amplitudes of the exciting waves. As the amplitudes of the exciting waves increase, effects higher than second order will become noticeable, giving waves at frequencies $3f_1$, $3f_2$, $2f_1 \pm f_2$, and so on.

The theory of Pekarek and others has had considerable success in explaining the characteristics of striations. This theory is a linear theory, however, and since most striations are of large amplitude, the nonlinear effects should influence the striation's

behavior considerably. We hope that this theory will result in better agreement with the low-amplitude waves, and will predict the second-order nonlinear effects.

2. Apparatus

A hot-cathode glow discharge is run in helium or argon in a discharge tube with 4-cm diameter. Pressures are usually between 0.1 Torr and 1.0 Torr, with currents from 30 mA to 150 mA. The plasma density is 10^{10}-10^{11} particles per cm^3, with an axial electric field of 1-4 V/cm. Electron thermal energy is from 3 eV to 8 eV in Helium, and from 1 eV to 2 eV in Argon.

Total tube length is 120 cm. At approximately the midpoint are 2 grids made of tungsten mesh, spot-welded to stainless-steel rings that fit the inside diameter of the tube. The grids are spaced 5 cm apart axially. The discharge runs from the cathode to an anode, passing through the grids. The grids have usually been left at their floating potential, but DC current can be drawn from them if desired.

A sine wave from an oscillator fed to one of the grids will cause a wave to be launched in the plasma. The boundary conditions at the grid are not known, but there is fairly strong coupling to the plasma. The waves in the plasma are detected by Langmuir probes spaced at intervals in the plasma. The probes may be used to detect variations in the plasma potential or, by biasing them properly, electron or ion density changes may be detected. Typically, a 2-V signal applied to a grid may produce a 1-1.5 V response at a probe 40 cm from the grid. The frequencies used, thus far, have been from 1 kHz to 30 kHz. The pressure and current are so chosen that there are no self-sustaining striations in the plasma, whenever this is possible.

To determine the nonlinear effects, the 2 grids are driven at different frequencies, and the amplitudes of the sum and difference frequencies are measured. As expected from theory, their amplitude is proportional to the product of the driven wave amplitudes. For example, for driving frequencies of 20 kHz and 30 kHz if we define G by $A\,(10\text{ kHz}) = G \times A\,(20\text{ kHz}) \times A\,(30\text{ kHz})$, where A is the amplitude of the signal, then $G = 100\text{ mv/(volt)}^2$ for He at 0.35 Torr. Reproducibility from day to day of the value of G is ±50%, but the quadratic relationship of the equation above is followed very precisely.

Thus, the effect looked for has been seen experimentally. There are, however, several important questions to be answered. First, where does the nonlinearity that causes the sum and difference frequency signals occur? The detection system has been checked and found to have nonlinearities much smaller than the observed signals, so the effect is actually coming from the discharge tube. Recent experiments in which the DC potential of the grids has been varied indicate that changing the potential (and in the process changing the DC current) of the grids has a large effect on the value of G. This may indicate that some or all of the nonlinear signal may be generated in the sheaths around

the grids, although nothing certain can be said yet. Work is continuing to try to answer this question, and to measure the properties of the linear waves more precisely.

D. W. Swain

C. REFRACTIVE ATTENUATION OF RADIATION IN A CYLINDRICAL PLASMA

In traversing a nonuniform plasma a radiation beam can be attenuated not only by plasma absorption, reflection, and scattering but also by refraction, which distorts the transmitted beam. Since light rays propagating in a plasma are bent by nonuniformities in the plasma refractive index, a portion of the radiation beam may be bent sufficiently by the plasma to cause it to miss a radiation detector that it would otherwise reach, or to reach a detector that it would otherwise miss.

This report describes a calculation of the refractive attenuation in a cylindrically symmetric plasma column in which the refractive index is a function only of the radial distance from the axis of symmetry. In particular, the refractive index corresponds to

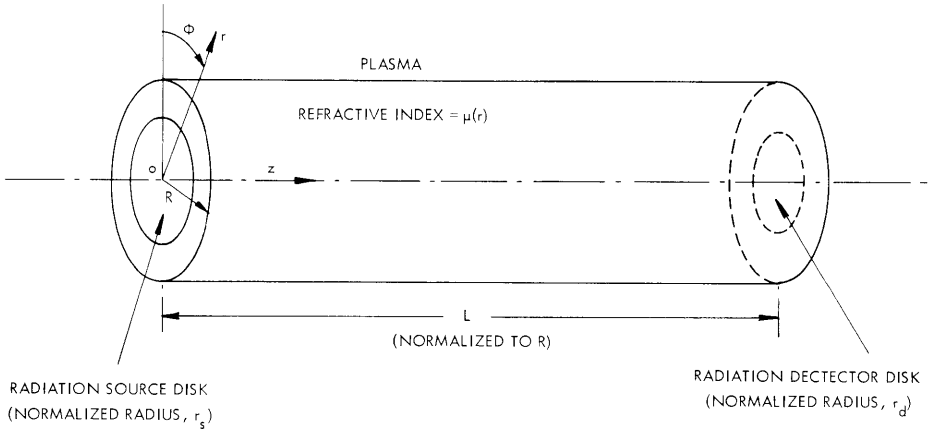

Fig. X-3. Cylindrically symmetric plasma column with radiation source and detector.

a parabolic electron density distribution with an adjustable radial density gradient. Figure X-3 illustrates the physical model for the calculation, in which all space variables, such as the radial and axial coordinates r and z, and the plasma length L, are normalized to the cylinder radius R.

The radiation source is a diffuse (or Lambertian) radiator in the form of a disk of radius r_s centered at one end of the plasma cylinder. The radiation detector is a disk of radius r_d centered at the other end of the plasma cylinder. The radiation reaching

this detector from the diffusely radiating disk source approximates a radiation beam in an optical system in which (i) the radiation source is a diffuse radiator; and (ii) the field stop and the aperture stop are imaged at opposite ends of the plasma cylinder, with the dimensions of the stop images being equal to the dimensions of the disks at their respective ends of the cylinder. The detector response is assumed to be independent of position on the detector surface and angle of incidence of incoming radiation. Such a response approximates that of a radiation detection system in which a light pipe directs the radiation to a detecting element.

If P is the radiant power reaching the detector from the disk source, then the transmittance of the plasma, T, is given by

$$T = \frac{P_p}{P_o} = e^{-\tau}, \tag{1}$$

where the subscripts p and o indicate the presence and absence of the plasma, respectively, and τ represents the effective optical depth of the plasma. Only radiation that reaches the detector directly from the source without reflection from any surface or boundary is considered.

Geometrical optics is used throughout this calculation. This approach is valid if the refractive index, μ, varies slowly with position, changing little over a distance equal to the wavelength of the radiation in the medium λ_m. This criterion is expressed as

$$\left(\frac{\lambda_m}{\mu}\frac{d\mu}{ds}\right) \ll 1, \tag{2}$$

where ds is an element of distance, and the wavelength in the medium λ_m is given in terms of the free-space wavelength λ as $\lambda_m = (\lambda/\mu)$. Diffraction effects are ignored.

In the following discussion the position of a point in a ray trajectory is given by the coordinates r, θ, z. The direction of a ray at any point in its trajectory is given by ψ, the angle between the ray tangent and the z-axis, and ϕ, the angle between the projection of the ray tangent on the transverse plane and the radius vector. The subscript o will refer to values of ray parameters at the source plane (z=0).

The radiant power reaching a surface element da_d of the detector from a surface element da_s of the source – with or without a plasma present – is given by

$$dP = I \cos \psi_o da_s (d\Omega)_d, \tag{3}$$

where I is the (constant) radiance of the source, $(d\Omega)_d$ is the solid angle subtended at da_s by the elementary bundle of rays that proceed to da_d (after some bending, if the plasma is present), and ψ_o is the angle between the direction of the elementary ray bundle at da_s and the normal to da_s (the z-axis). The cos ψ_o term is required because the source is

a diffuse radiator. Since

$$da_s = r_o d\theta_o dr_o \tag{4}$$

and

$$(d\Omega)_d = \sin \psi_o d\psi_o d\phi_o, \tag{5}$$

where ϕ_o is the angle at da_s between the radius vector and the projection onto the transverse plane of the ray that defines the direction of the elementary ray bundle, Eq. 3 can be rewritten

$$dP = I \cos \psi_o (r_o d\theta_o dr_o)(\sin \psi_o d\psi_o d\phi_o). \tag{6}$$

Integrating over the surfaces of the source and detector yields

$$P = 2\pi I \int_0^{r_s} r_o \, dr_o \int_{a_d} \sin \psi_o \cos \psi_o \, d\psi_o d\phi_o, \tag{7}$$

where, for each r_o, the second integral is performed over the entire surface of the detector. Equation 7 can be rewritten

$$P = \pi I \int_0^{r_s^2} S(r_o) \, d\left(r_o^2\right), \tag{8a}$$

where

$$S(r_o) = \int_{\phi_o} \int_{\psi_o} d\left(\sin^2 \psi_o\right) d\phi_o. \tag{8b}$$

In Eq. 8b, ψ_o, ϕ_o, and r_o are coupled by the trajectory equations for rays that reach the detector from a surface element of the source at a distance r_o from the axis; r_o, ψ_o, and ϕ_o represent the initial conditions in these equations. For a given r_o, these trajectory equations yield a functional relationship between ψ_o and ϕ_o for rays that reach the boundary of the detector, and it is this functional relationship that gives the limits of integration for Eq. 8b.

To obtain the plasma transmittance, as given by Eq. 1, Eq. 8 must be evaluated with both a nonuniform plasma refractive index present between the source and detector (P_p), and a uniform refractive index of unity present (P_o). Clearly, in the latter case the ray trajectories are simply straight lines. An expression for P_o is already available,[1,2] and it is

$$P_o = \frac{I\pi^2}{4} \left\{ \sqrt{L^2+(r_d+r_s)^2} - \sqrt{L^2+(r_d-r_s)^2} \right\}^2. \tag{9}$$

The calculation of P_p, however, requires an analysis of the ray trajectory equations.

1. Ray Trajectory– General

The ray trajectories are described by equations giving r and θ as functions of z for a given set of initial ray parameters (r_o, ψ_o, ϕ_o). For the present geometry the relevant equation is[3,4]

$$dz = \pm \frac{Ardr}{(\mu^2 r^2 - A^2 r^2 - B^2)^{1/2}}, \tag{10}$$

where A and B are "constants of motion" given by

$$A = \mu \cos \psi = \mu_o \cos \psi_o \tag{11}$$

$$B = \mu r \sin \phi \sin \psi = \mu_o r_o \sin \phi_o \sin \psi_o, \tag{12}$$

and the plus or minus sign is taken if the ray is proceeding toward a larger or smaller radius, respectively. A similar equation for θ is available but will not be used here, since only information on the radial positions of rays at the detector plane is required; their azimuthal positions are of no significance.

For an infinitely long cylinder all rays (except the ray along the axis) consist of two symmetric halves about a point where r is a minimum. The value of this distance of closest approach to the axis r_m is obtained by setting the denominator of Eq. 10 equal to zero, which corresponds to (dr/dz) = 0. That is,

$$\mu^2 r_m^2 - A^2 r_m^2 - B^2 = 0. \tag{13}$$

Before reaching r_m along a ray, the minus sign in Eq. 10 is used; after r_m, the plus sign is used.

A finite cylinder may be considered part of a longer cylinder. Thus, if, for a given ray, r_m is located within the finite length, then the sign of Eq. 10 changes at the location of r_m along the cylinder.

2. Plasma Refractive Index

If ν/ω, $\omega_b/\omega \ll 1$, where ω is the radian frequency of the radiation, ν is the collision frequency of electrons with other particle species, and ω_b is the electron cyclotron radian frequency, then the plasma refractive index is given by

$$\mu^2 = 1 - \frac{n}{n_c}, \qquad \frac{n}{n_c} < 1, \tag{14}$$

where n is the electron density, and n_c is the critical or cutoff density at the frequency of interest (the density for which ω is the plasma frequency). For a parabolic density distribution

$$n = n_o(1-\alpha r^2), \tag{15}$$

where the constant α (>0) determines the degree of nonuniformity of the electron density, and n_o is the central density, the refractive index becomes

$$\mu^2 = (1-\eta) + (\eta\alpha)r^2, \tag{16}$$

where

$$\eta = \frac{n_o}{n_c} = (8.96\times10^{-16})\lambda^2 n_o, \qquad \lambda, \text{ mm}; \quad n_o, \text{ cm}^{-3}. \tag{17}$$

Here, λ is the free-space wavelength of the radiation.

Note that since μ decreases toward the axis, the plasma acts like a diverging lens.

3. Ray Trajectory for Parabolic Density Distribution

The ray trajectory equations are obtained by substituting Eq. 16 in Eq. 10 and integrating. The parabolic distribution is one of the few distributions for which Eq. 10 can be integrated. Because of the double sign, the resulting ray equations are of three forms, determined by whether the axial location of the minimum radius of the ray is before the source plane, between the source and detector, or after the detector plane. The resulting equations are

$$L = \begin{cases} Z_{d,m} - Z_{o,m}; & \phi_o < \pi/2 & \text{(18a)} \\ Z_{o,m} + Z_{d,m}; & \phi_o > \pi/2, \quad Z_{o,m} < L & \text{(18b)} \\ Z_{o,m} - Z_{d,m}; & \phi_o > \pi/2, \quad Z_{o,m} > L & \text{(18c)} \end{cases}$$

where

$$Z_{o,m} = \frac{1}{2}\left[\left(\frac{1}{\gamma} + r_o^2\right)\cos^2\psi_o\right]^{1/2} \ln\left|\frac{2\left(\rho_o \sin^2\psi_o \cos^2\phi_o\right)^{1/2} + \rho_o + \sin^2\psi_o}{\left[\left(\sin^2\psi_o - \rho_o\right)^2 + 4\rho_o \sin^2\psi_o \sin^2\phi_o\right]^{1/2}}\right| \tag{19a}$$

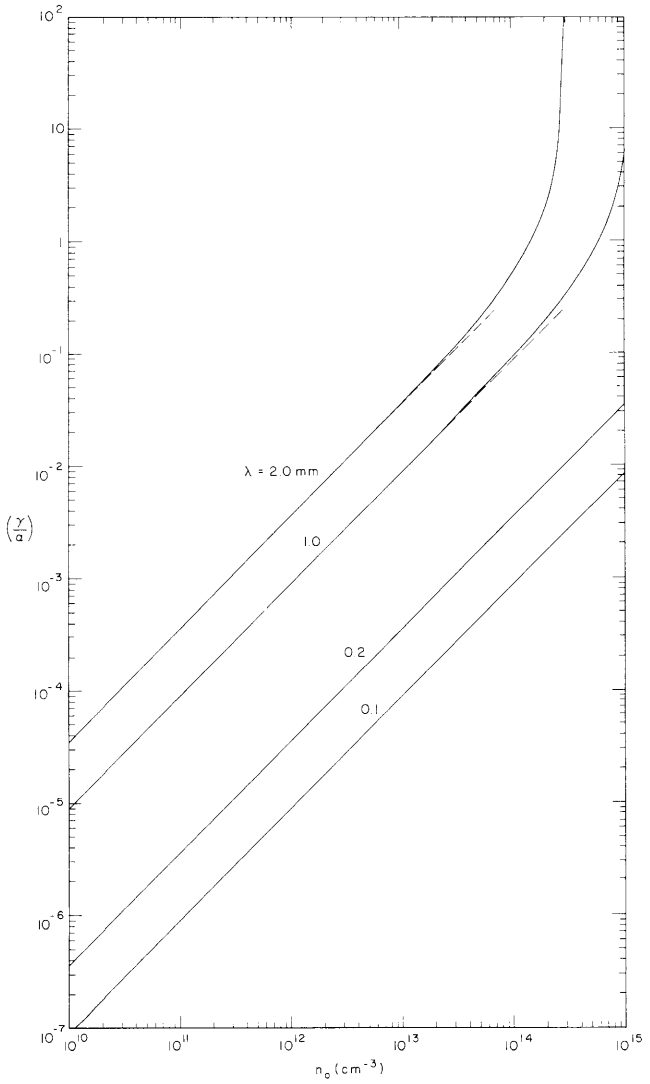

Fig. X-4. (γ/a) as a function of central electron density for several mm and sub-mm wavelengths.

$$Z_{d,m} =$$

$$\frac{1}{2}\left[\left(\frac{1}{\gamma}+r_o^2\right)\cos^2\psi_o\right]^{1/2} \ln\left|\frac{2\left[\rho_d^2+\rho_d\left(\sin^2\psi_o-\rho_o\right)-\rho_o\sin^2\psi_o\sin^2\phi_o\right]^{1/2}+2\rho_d+\sin^2\psi_o-\rho_o}{\left[\left(\sin^2\psi_o-\rho_o\right)^2+4\rho_o\sin^2\psi_o\sin^2\phi_o\right]^{1/2}}\right| \tag{19b}$$

and

$$\gamma = \left(\frac{\eta a}{1-\eta}\right) \tag{20}$$

$$\rho_o = \frac{r_o^2}{\left(\frac{1}{\gamma}+r_o^2\right)}, \qquad \rho_d = \frac{r_d^2}{\left(\frac{1}{\gamma}+r_o^2\right)}. \tag{21}$$

Equations 18 can be rewritten to express ρ_d, $\cos\phi_o$, and $\sin\psi_o$ separately in terms of the other quantities. These forms of the ray equations are useful in the final computation.

Note that both parameters characterizing the plasma properties (η for the axial electron density, and a for the radial decay rate of the density) enter the ray trajectory equations only through the single constant, γ. From Eqs. 17 and 20, γ is given by $\frac{\gamma}{a} = \left(\frac{n_o}{n_c - n_o}\right)$. Figure X-4 illustrates how (γ/a) depends on n_o for several wavelengths in the mm and sub-mm ranges; a is generally of order unity. For $n_o \ll n_c$, γ/a varies linearly with n_o; as n_o approaches n_c, γ/a increases rapidly.

4. Plane Wave (Parallel Ray) Approximation

The mathematical problem is greatly simplified if, instead of a diffusely radiating source, we consider a source that emits only rays parallel to the cylinder axis. Although such a source cannot exist in reality, it might be a reasonable approximation for laser radiation. Also, such a "plane wave" source corresponds to an approximation frequently used for illumination not nearly as collimated as laser light.

The mathematical problem is reduced to the determination of a "critical radius," r_c, which is the radius in the source plane from which a ray that is initially parallel to the axis just reaches the edge of the detector. All rays from $r_o < r_c$ reach the detector, and all those from $r_o > r_c$ miss it. Thus if the disk source radiates uniformly over its surface and $r_d < r_s$, then the radiant power reaching the detector with and without

the plasma present is $P_p = I\pi r_c^2$ and $P_o = I\pi r_d^2$, respectively, where I is the power per unit area emitted by the source. The resulting transmittance is

$$T_p = r_c^2/r_d^2, \qquad r_d < r_s \tag{22}$$

where the subscript p refers to the parallel ray approximation. (The corresponding effective optical depth of the plasma is τ_p.) If $r_d > r_s$, then if $r_c < r_s$, the transmittance is

$$T_p = \frac{P_p}{P_o} = \frac{I\pi r_c^2}{I\pi r_s^2} = \frac{r_c^2}{r_s^2} \qquad r_d > r_s, \quad r_c < r_s \tag{23}$$

and if $r_c > r_s$, the transmittance is

$$T_p = \frac{P_p}{P_o} = \frac{I\pi r_s^2}{I\pi r_s^2} = 1 \qquad r_d > r_s, \quad r_c > r_s. \tag{24}$$

The radius r_c is given by setting $r_o = r_c$ and $\sin\psi_o = 0$ in Eq. 18a or Eq. 18b, which, after some algebraic manipulation, yields

$$L = \left(\frac{1}{\gamma} + r_c^2\right)^{1/2} \ln\left|\left(\frac{\rho_d}{\rho_c}\right)^{1/2} + \left(\frac{\rho_d}{\rho_c} - 1\right)^{1/2}\right|. \tag{25}$$

This equation can be solved for $\left(\frac{\rho_d}{\rho_c}\right)$ to give

$$\frac{\rho_d}{\rho_c} = \cosh\left[\frac{L}{\left(\frac{1}{\gamma} + r_c^2\right)^{1/2}}\right]. \tag{26}$$

5. Computer Calculation

A computer program has been written to calculate the transmittance for the diffuse-radiator case (T) and the parallel-ray case (T_p). For the calculation of T, Eq. 8a is computed in two parts, one for $r_o < r_c$, the other for $r_o > r_c$, with r_c being computed from Eq. 26 by iteration. For $r_o < r_c$ the cone of rays from each source point contains the ray perpendicular to the source. Consequently, the ϕ_o integration extends simply from 0 to 2π, and the values of $\sin^2\psi_o$ for different values of ϕ_o are calculated from Eqs. 18a and 18b by iteration. Equation 18c does not apply in this case.

For $r_o < r_c$, however, the cone of rays from each source point does not contain the source normal. In this case the limits of integration of $\sin^2\psi_o$ are first calculated by

iteration. Equation 18b applies for the larger limit, since the ray must pass through its minimum radius before reaching the detector edge. For the smaller limit either Eq. 18b or Eq. 18c applies. In the computer program, however, the solutions of Eqs. 18 for ρ_d are used for calculating both limits of integration. With the limits of $\sin^2 \psi_o$ computed, the values of ϕ_o for intermediate values of $\sin^2 \psi_o$ are calculated by using the solutions of Eqs. 18 for $\cos \phi_o$.

Since r_c is calculated in the computation of T, it is available for the computation of T_p with no significant additions to the program.

6. Computation Results

The values of T and T_p for $r_s^2 = 0.8$, $r_d^2 = 0.15$, L = 20 are plotted in Fig. X-5 as a function of γ. In general, T_p is considerably less than T. This is not unreasonable, since in the parallel ray approximation all rays are bent away from the axis by the plasma, and consequently they reach the detector at larger radii than they do with no

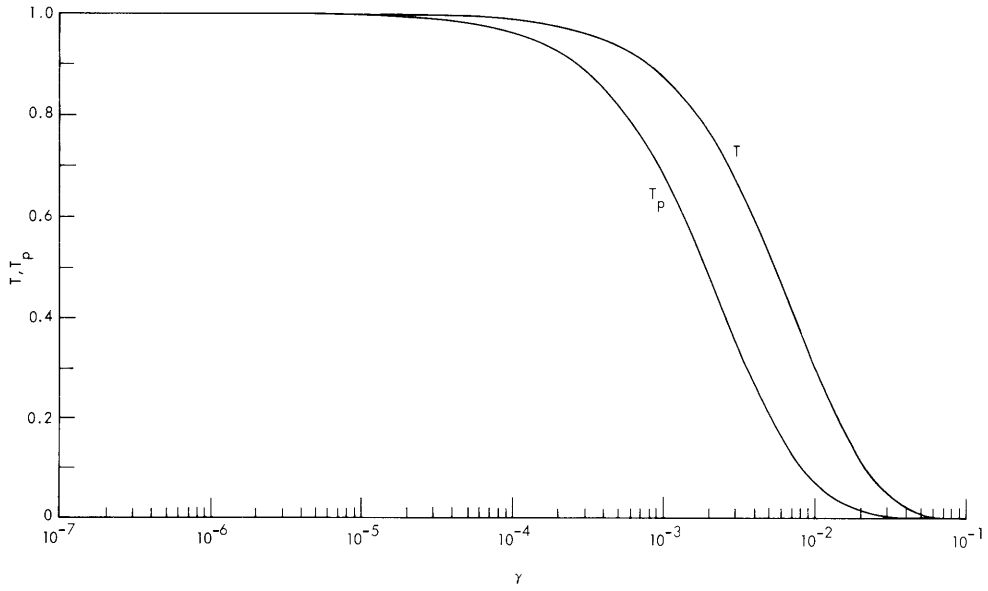

Fig. X-5. Plasma transmittance as a function of γ for diffuse radiator (T) and plane-wave radiator (T_p) for $r_s^2 = 0.8$, $r_d^2 = 0.15$, L = 20.

plasma present. With a diffuse source, on the other hand, some rays are bent toward the axis, in the sense that they arrive at the detector at smaller radii than they do without the plasma. Thus some rays that would miss the detector with no plasma present are actually bent toward the detector by the plasma. For values of γ in the range $\sim 5 \times 10^{-5}$-$\sim 5 \times 10^{-2}$ the plane wave approximation (T_p) is clearly a poor substitute for

the exact calculation (T). For the "absorption" (1-T) the range of γ for which the plane-wave case is a poor approximation extends farther toward smaller values.

An interesting and unexpected result of the computation involves the independence of the transmittance and optical depth on the detector radius r_d. T, T_p, τ, and τ_p have been calculated for $r_d^2 = 0.3,\ 0.15,\ 72,$ for $\gamma = 10^{-7}, 10^{-6}, \ldots, 10^{-1}$ with fixed $r_s^2 = 0.8$. The spread in the results for all four quantities is less than 0.001 — in most cases considerably less. Thus, for the range of γ and r_d specified, the values of the transmittance and optical depth are effectively independent of detector size.

This result is consistent with the fact that the closer rays are to the plasma axis, the less they are bent, since the electron density gradient decreases with decreasing radius. Thus rays reaching a small detector are on the average bent less than those reaching a large detector, since more of the former rays travel near the axis than do the latter.

The computation was carried out on the IBM System 360 computer at the Computation Center, M.I.T.

G. L. Rogoff

References

1. M. Von Rohr (ed.), Geometrical Investigation of the Formation of Images in Optical Instruments, Vol. I of The Theory of Optical Instruments (H. M. Stationery Office, London, 1920), pp. 523-524.

2. A. Beers, Grundriss Des Photometrischen Calcüles (Friedrich Vieweg u. Sohn, Brunswick, 1854), pp. 61-62.

3. M. A. Heald, "Tracing of Oblique Rays in Plasma Cylinders," Report CLM-R34, U.K. Atomic Energy Authority, 1964. Note: The ray trajectory angles ψ and ϕ used in the present report are related to the angles in Heald's report as follows: $\psi = \pi/2 - \omega$, where ω is used in Heald's report; ϕ is the same as in Heald's report.

4. Y. Aoki, "Light Rays in Lens-like Media," J. Opt. Soc. Am. 56, 1648-1651 (1966).

D. STOCHASTIC ACCELERATION IN BOUNDED PLASMAS

1. Introduction

One often observes production of high-energy particles in laboratory plasmas. One attractive explanation for this phenomenon is that there are turbulent fields in the plasma which stochastically accelerate a few electrons to high energy. In both quasi-linear theory and Dupree's strong-turbulence theory, however, the maximum velocity to which a particle may diffuse in velocity space is limited by the maximum phase velocity of the turbulent waves. For instance, in one-dimensional quasi-linear diffusion theory,[1] the diffusion constant has the $\delta(kv-\omega)$ resonance. Thus particles traveling faster than the fastest phase speed cannot be diffused. In Dupree's strong-turbulence theory,[2] which

may be looked upon roughly as a trapping theory, this resonance acquires a finite width. This width is the so-called trapping width of the potential, equal to $\sqrt{2eE/mk}$, where E is the rms electric field, and k is a typical wave number of the turbulent spectrum. Thus diffusion is still limited by the phase velocity, although particles can be diffused somewhat beyond the maximum phase velocity in the wave spectrum. Thus it appears that stochastic acceleration theory in one dimension is not capable of explaining the production of high-energy particles, as long as the turbulent waves have only a finite phase velocity. One method of stochastic acceleration that appears to circumvent this restriction involves the acceleration of a particle in a single wave whose phase varies randomly in time.[3-5] It has been shown that if the waveform has this property, particles can be accelerated to much higher velocity than the waves' phase velocity. These sudden random phase changes in the waveform imply infinite frequencies, however, and thus infinite phase velocities, so there is no contradiction with quasi-linear theory.

A measurement of the frequency spectrum in any plasma will determine whether or not this model is realistic. In many cases, the frequency spectrum of the turbulence has definite, measurable upper limits, which implies that there can be no sudden phase changes.

Although many effects come into play in a laboratory experiment, it is significant that production of high-energy particles is observed in at least two sets of computer experiments. Here the plasmas are one-dimensional homogeneous plasmas. First, Dawson[6] used a charge-sheet model to test the quasi-linear theory of the "bump on tail" instability. He found that the bump flattened in accordance with the predictions of quasi-linear theory, but for a long time afterward he observed particles whose velocity is much greater than the original beam velocity.

Second, Bers and Davis[7,8] also used a charge-sheet model to investigate a beam plasma instability. They found that a field strong enough to trap some of the plasma electrons is initially set up at one point in space. A long time later, however, the distribution of trapped electrons was observed to have a characteristic width in velocity space much larger than the "trapping width" of the wave.

In this report, we shall investigate a mechanism by which these high-velocity particles may be produced. What is involved is the finiteness of the system. Let us say the system is of length ℓ. If a group of particles of velocity v pass through the system, they emerge with a distribution of velocities having some characteristic spread $<\delta v>$. If these particles can somehow be reintroduced into the system, they will spread out farther in velocity space. After they have passed through the system n times, the characteristic spread will be roughly $n<\delta v>$. This will be true whether or not the particles are resonant with the waves. The only effect particle-wave resonance can have is to make $<\delta v>$ larger for particles that are resonant, and smaller for particles that are not. Thus particles initially in resonance can diffuse out of resonance. If after n transits

$n < \delta v >$ remains small, we can write out a Fokker-Planck equation for the distribution $f(v)$ as a function of n, the number of transits.

We shall consider the quasi-linear limit; that is, when δv can be determined by orbit perturbation theory. It turns out that the Fokker-Planck equation is a diffusion equation for nonresonant particles, but not for resonant particles.

We shall also consider the trapping limit; that is, in some inertial frame, the waveform has a constant profile. Thus, either a trapped or untrapped particle is acted upon by a stationary random potential. The problem here is much more difficult, but with very rough approximations, one may still write down a diffusion equation for f.

2. Quasi-linear Limit

Let us consider a one-dimensional plasma of length ℓ supporting weakly turbulent electrostatic fluctuations. We assume periodic boundary conditions so that when a particle exits one end of the system, it enters the other end. The waves will be assumed to have phase velocities between u_1 and u_2.

We assume now that the turbulence is so weak that a particle can make several transits through the system without changing its velocity very much. Second, we assume that the autocorrelation time of the fields is much less than ℓ/v, the transit time for a particle. Thus the field on each transit is uncorrelated from the field of the previous transit. Under these assumptions, the distribution of particle velocity as a function of n, the number of transits through the system, obeys a Fokker-Planck equation

$$\frac{\partial f}{\partial n} = \frac{1}{2} \frac{\partial^2}{\partial v^2} \frac{\langle \Delta v^2 \rangle}{\Delta n} f - \frac{\partial}{\partial v} \frac{< \Delta v >}{\Delta n} f. \tag{1}$$

Thus the problem reduces to finding the Fokker-Planck coefficients.

Let us define the random variable δv as the change in particle velocity after one transit. If the fields are sufficiently weak, the average and variance of δv can be found by orbit perturbation theory. That is, if the electric field is $E(x, t)$, to first order the change in particle velocity at time t is given by

$$v_1 = \int_0^t \frac{e}{m} E(x+vt', t')\, dt'. \tag{2}$$

The first approximation to the variance of δv is then given by

$$\left\langle v_1^2 \right\rangle = \int_0^t dt' \int_0^t dt'' \frac{e^2}{m^2} \left\langle E(x+vt', t') E(x+vt'', t'') \right\rangle = \int_0^t dt' \int_0^t dt'' \frac{e^2}{m^2} E^2(v(t'-t''), t'-t''), \tag{3}$$

where E^2 is the space-time correlation function of the electric field.

To calculate the average of δv, we must go to second order in perturbation theory

because the average of Eq. 2 is zero, since $\langle E \rangle = 0$. The equation of motion of a particle can be iterated once more to give

$$v_2(t) = \left\langle \int_0^t \frac{e}{m} x,(t') \frac{\partial}{\partial x} E(x+vt', t') \right\rangle ; \tag{4}$$

however,

$$x,(t') = \int_0^{t'} dt'' \int_0^{t''} dt''' \frac{e}{m} E(x+vt''', t''') = \int_0^{t'} dt'' \frac{e}{m} (t'-t'') E(x+vt'', t''). \tag{5}$$

Then Eq. 4 can be rewritten

$$\left\langle v_2 \right\rangle = \int_0^t dt' \int_0^{t'} dt'' \frac{e^2}{m^2} \left\langle (t'-t'') E(x+vt'', t'') \frac{\partial}{\partial v(t'-t'')} E(x+vt''+v(t'-t''), t''+(t'-t'')) \right\rangle$$

$$= \int_0^t dt' \int_0^{t'} dt'' \frac{e^2}{m^2} \frac{\partial}{\partial v} E^2(v(t'-t''), t'-t''). \tag{6}$$

Since the correlation function must be an even function of $t'-t''$, the expression may be rewritten

$$\left\langle v_2 \right\rangle = \frac{1}{2} \int_0^t dt' \int_0^t dt'' \frac{e^2}{m^2} \frac{\partial}{\partial v} E^2(v(t'-t''), t'-t''). \tag{7}$$

For any time t, it is clear that $\left\langle v_1^2(v, t) \right\rangle$ and $\left\langle v_2(v, t) \right\rangle$ are related by

$$\frac{1}{2} \frac{\partial}{\partial v} \left\langle v_1^2(v, t) \right\rangle = \left\langle v_2(v, t) \right\rangle . \tag{8}$$

But, in Eqs. 7 and 3, t is the transit time, and it is itself a function of v, $t = \ell/v$. Thus in general

$$\frac{1}{2} \frac{\partial}{\partial v} \left\langle v_1^2(v) \right\rangle \neq \left\langle v_2(v) \right\rangle . \tag{9}$$

Equation 9 becomes an equality, however, as long as both $\left\langle v_1^2 \right\rangle$ and $\left\langle v_2 \right\rangle$ are not functions of time. The expressions $\left\langle v_2 \right\rangle$ and $\left\langle v_1^2 \right\rangle$ are both functions of v. If the electric field is weak enough so that after n transits $\sum_{i=1}^{n} \delta v$ is small compared with the characteristic scale on which they vary, $\left\langle v_2 \right\rangle$ and $\left\langle v_1^2 \right\rangle$ may be regarded as independent of v. Then, by the central limit theorem,[9] we may conclude that the distribution of $\Delta v = \sum_{i=1}^{n} \delta v_i$ is Gaussian, with mean $n \left\langle v_2 \right\rangle$ and variance $n \left\langle v_1^2 \right\rangle$. Indeed if the

distribution of E is Gaussian, so is the distribution of v_1, since it is obtained by only linear operations on E. Therefore, the convergence of $P(\Delta v)$ to a Gaussian is probably fairly rapid.

Thus the Fokker-Planck equation given by Eq. 1 is simply

$$\frac{\partial f}{\partial n} = \frac{1}{2} \frac{\partial^2}{\partial v^2} \left\langle v_1^2 \right\rangle f - \frac{\partial}{\partial v} \left\langle v_2 \right\rangle f. \tag{10}$$

All that we need do now is calculate the Fokker-Planck coefficient given by Eqs. 3 and 7. Let us say that the electric field is given by

$$E(x,t) = \mathrm{Re} \sum_k E(k)\, e^{i(kx-\omega_k t+\phi_k)}, \tag{11}$$

where ω_k is related to k by the dispersion relation, and ϕ_k is the random phase associated with the wave at k. The wave spectrum will be assumed to be restricted to phase velocities between u_1 and u_2.

Then from Eq. 11 we may write

$$E^2(v(t'-t''), t'-t'') = \mathrm{Re} \sum_k |E(k)|^2 e^{i(kv-\omega)(t'-t'')}. \tag{12}$$

Thus

$$\left\langle v_1^2 \right\rangle = \frac{e^2}{m^2} \sum_k |E(k)|^2 \frac{\sin^2\left(\frac{kv-\omega}{2}\right)\frac{\ell}{v}}{\left(\frac{kv-\omega}{2}\right)^2} \tag{13}$$

and

$$\left\langle v_2 \right\rangle = \frac{e^2}{m^2} \frac{\partial}{\partial v} \sum_k |E(k)|^2 \left. \frac{\sin^2\left(\frac{kv-\omega}{2}\right)\frac{\ell}{v'}}{\left(\frac{kv-\omega}{2}\right)^2} \right|_{v'=v}. \tag{14}$$

Let us plot the diffusion constant $D = 1/2 \left\langle v_1^2 \right\rangle$ as a function of velocity. In the resonant region, $u_1 < v < u_2$,

$$D = \frac{\pi e^2}{m^2} \frac{\ell}{v} \sum_k |E(k)|^2 \delta(kv-\omega),$$

the ordinary quasi-linear diffusion constant evaluated at $t = \ell/v$. In the nonresonant region,

$$D \approx \frac{1}{2} \frac{e^2}{m^2} \sum_k \frac{|E(k)|^2}{\left(\frac{kv-\omega}{2}\right)^2},$$

where we have made use of the fact that $\left\langle \sin^2 (kv-\omega)\frac{\ell}{v} \right\rangle = \frac{1}{2}$. A plot of D as a function of v is shown in Fig. X-6. Notice that outside the resonant region $v_1^2(v,t)$ is

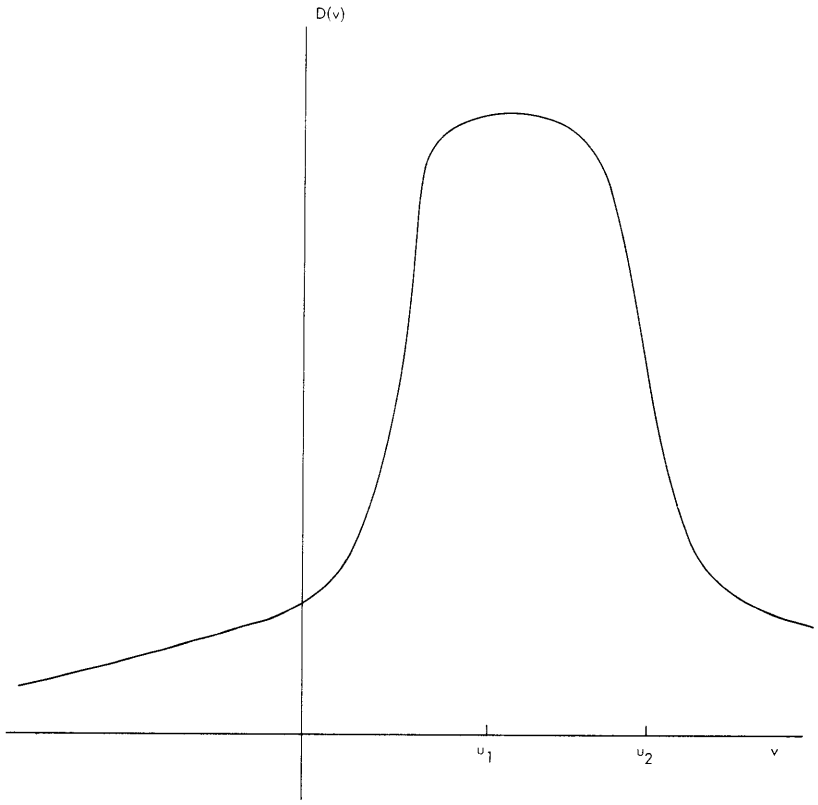

Fig. X-6. D vs v.

not a function of t, so that outside of this region, the Fokker-Planck equation becomes a diffusion equation:

$$\frac{\partial f}{\partial n} = \frac{\partial}{\partial v} D \frac{\partial f}{\partial v}.$$

It is clear that diffusion is no longer restricted to those velocities coinciding with wave phase velocity. Thus, for a weak bump-on-tail instability in a one-dimensional plasma

with periodic boundary conditions, we expect a rapid flattening of the bump, followed by slow diffusion of particles outside the region of the bump. Since periodic boundary conditions are assumed, $\Delta n = v\Delta t/\ell$, and the Fokker-Planck equation outside the resonant region can be written in time as

$$\frac{\partial f}{\partial t} = \frac{1}{2}\frac{v}{\ell}\frac{\partial}{\partial v}\left\langle v_1^2 \right\rangle \frac{\partial f}{\partial v}. \tag{15}$$

3. Particle Acceleration in a Constant Profile Wave

Now let us consider another possibility, namely that in the system of length ℓ a disturbance of constant profile propagates through the system with speed v_{ph}. We are interested in the distribution of particle velocities after the particle has passed n times through the system in the direction of v_{ph}. We assume that ℓ/v_{ph} ~ transit time » typical trapping time in the potential wells of the constant profile wave. Also, we shall work in the frame in which the wave is at rest.

It will turn out that this problem is much more difficult than the quasi-linear problem treated above. But with very rough approximations we can glean some insight into the behavior of the particle distribution function. Qualitatively, the results are the same, namely that particles can be diffused even if they are not within the "trapping width" of the wave. The mechanism is basically the same. A trapped or untrapped particle is acted upon by the potential until its final velocity becomes uncorrelated with its initial velocity. Then, when the particle is reflected, it is reintroduced into the waveform at some random potential, and its velocity can change further. In this way, a particle velocity can change beyond the "trapping reach" of the wave; however, during any transit the velocity is always between

$$\sqrt{\frac{2}{m}}\sqrt{\frac{1}{2}mv_o^2 + (\phi_o - \phi_{min})} < v < \sqrt{\frac{2}{m}}\sqrt{\frac{1}{2}mv_o^2 + (\phi_{max} - \phi_o)},$$

where v_o is the initial velocity, ϕ_o is the initial potential energy, and ϕ_{max} and ϕ_{min} are the maximum and minimum potential present in the waveform.

Let us say that the probability that the potential energy in the waveform is between ϕ and $\phi + d\phi$ is given by $P(\phi)\,d\phi$, where $\int P(\phi)\,d\phi = 1$. We also assume that in one very long waveform of length L, $P(\phi)\,d\phi$ is equal to dx/L, where dx is the length of space corresponding to potentials between ϕ and $\phi + d\phi$.

Let us say that at some time a particle is introduced at velocity v_o and potential ϕ_o. We would like the probability that a long time later the particle is between potential ϕ and $\phi + d\phi$. This problem has been solved by T. S. Brown,[10] and we will reproduce his solution here. The probability that is sought is simply the fraction of time that the particle spends between these two potentials. This time is the total distance dx when the potential is between ϕ and $\phi + d\phi$, divided by the particle velocity.

Thus the relative probability that an untrapped particle sees potential ϕ is simply

$$\frac{P(\phi)\, d\phi}{\sqrt{\frac{2}{m}}\sqrt{\frac{1}{2}mv_o^2 + \phi_o - \phi}}.$$

For a trapped particle, certain regions of space are forbidden to the particle, since the potential energy must be less than the total energy.

For trapped particles, the probability that the particle experiences the potential ϕ is

$$\frac{dx}{L'\sqrt{\frac{2}{m}}\sqrt{\frac{1}{2}mv_o^2 + \phi_o - \phi}},$$

where L' is the total distance along which the particle has traveled, and dx is the length along which the potential is between ϕ and $\phi + d\phi$.

Let us assume that $dx/L' = P'(\phi)\, d\phi$, where $P'(\phi)$ is proportional to $P(\phi)$ if the argument of the radical is positive, and $P'(\phi) = 0$ if the argument is negative. Of course, $P(\phi)$ is renormalized so that $\int P'(\phi)\, d\phi = 1$. In assuming that $dx/L' = P'(\phi)$, we are assuming that in regions of space corresponding to all trapped orbits, the potential has the same relative probability as it does in all space. Then for all particles, trapped as well as untrapped, the relative probability may be obtained by replacing $P(\phi)$ with $P'(\phi)$. Then the absolute probability that a particle will experience a potential ϕ is simply

$$\frac{\dfrac{P'(\phi)\, d\phi}{\sqrt{\frac{2}{m}}\sqrt{\frac{1}{2}mv_o^2 + \phi_o - \phi}}}{\int d\phi\, \dfrac{P'(\phi)\, d\phi}{\sqrt{\frac{2}{m}}\sqrt{\frac{1}{2}mv_o^2 + \phi_o - \phi}}}. \tag{16}$$

We shall now show that the quantity in the denominator is simply the reciprocal of the average of the magnitude of the particle velocity $\frac{1}{\langle |v| \rangle}$.

Let us note that the particle has a velocity as a function of position given by $v(x) = \sqrt{\frac{2}{m}}\sqrt{\frac{1}{2}mv_o^2 + \phi_o - \phi(x)}$. Also, $P'(\phi)\, d\phi$ is simply dx/L', where L' is the total distance a particle travels in its orbit. If the particle is trapped, L' is the total distance the particle travels both forward and backward. Then the denominator of (16) is simply $\left\langle \frac{1}{|v(x)|} \right\rangle$. Now it is a simple problem in kinematics to show that $\left\langle \frac{1}{|v(x)|} \right\rangle = \frac{1}{\langle |v| \rangle}$.

Let us note that the total time taken by the particle to travel the distance L' is simply

$t = L'/\left\langle |v| \right\rangle$. We may also write that t is the sum of all of the times that a particle spends in each region dx. Then

$$t = \int_0^{L'} \frac{dx}{|v(x)|}$$

and so

$$\frac{1}{\left\langle |v| \right\rangle} = \left\langle \frac{1}{|v(x)|} \right\rangle = \int d\phi \; \frac{P'(\phi)}{\sqrt{\frac{2}{m}} \sqrt{\frac{1}{2} mv_o^2 + \phi_o - \phi}}. \tag{17}$$

Thus the probability of observing the potential ϕ after a long time is given by

$$\frac{\left\langle |v| \right\rangle P'(\phi)\, d\phi}{\sqrt{\frac{2}{m}} \sqrt{\frac{1}{2} mv_o^2 + \phi_o - \phi}}. \tag{18}$$

From Eq. 18, we may write the probability that a particle has velocity between $|v|$ and $|v| + d|v|$ simply by noting that

$$\begin{aligned} \phi &= \tfrac{1}{2} mv_o^2 + \phi_o - \tfrac{1}{2} mv^2 \\ d\phi &= m|v|\, d|v|. \end{aligned} \tag{19}$$

Thus

$$P(|v|)\, d|v| = m\left\langle |v| \right\rangle \; P'\left(\tfrac{1}{2} mv_o^2 + \phi_o - \tfrac{1}{2} mv^2\right) d|v|. \tag{20}$$

Let us also note that $\left\langle |v| \right\rangle$, defined by Eq. 17, depends on v_o and ϕ_o, but not on v.

Now let us assume that after a particle passes once through the system it returns and starts out again with the velocity it had at $x = \ell$ and the potential that happens to be at $x = 0$. If a particle passes through the system n - 1 times, let us denote its distribution of velocity by $f_{n-1}(v)$. Then, from $f_{n-1}(v)$, $P(\phi)$, and Eq. 20, we can determine $f_n(v)$.

$$f_n(|v|) = \int d|v_i|\, d\phi_i\, m\left\langle |v| \right\rangle P'\left(\tfrac{1}{2} mv_i^2 + \phi_i - \tfrac{1}{2} mv^2\right) P(\phi_i)\, f_{n-1}(|v_i|). \tag{21}$$

If we integrate Eq. 17 to determine $\left\langle |v| \right\rangle$, in principle we can at least start with $f_o(v_i) = \delta(v)$ and iterate Eq. 7 to determine $f_n(|v|)$. Naturally, this is very difficult. It appears, however, correct, at least qualitatively, that $f_n(|v|)$ spreads out in velocity space with increasing n. Also, the trapping width $v_{tr} = \sqrt{\frac{2}{m}} \sqrt{\phi_{max} - \phi_{min}}$ is no restriction on

the spreading of $f_n(v)$ in velocity space. To gain any quantitative insight into the nature of Eq. 21, we shall make a few very gross assumptions. First, we assume $n \gg 1$ so that the distribution is quite spread over velocity, and its characteristic width is much greater than the trapping width. Therefore most of the particles are untrapped, and $E \gg \phi_{max} - \phi_{min}$, so $\left\langle |v| \right\rangle \approx v_i \approx v$. Also, for untrapped particles, $P' = P$. Therefore, Eq. 21 becomes

$$f_n(v) = \int dv_i d\phi_i \, mvP\left(\frac{1}{2} mv_i^2 + \phi_i - \frac{1}{2} mv^2\right) P(\phi_i) \, f(v_i), \tag{22}$$

where the absolute value signs on the v's have been deleted, since if the particles are untrapped, the final velocity is always in the same direction as the initial velocity.

Now to simplify things further, let us assume that $P(\phi)$ is Gaussian,

$$P(\phi) = \frac{1}{\sqrt{\pi}\,\Delta\phi} e^{-\frac{\phi^2}{(\Delta\phi)^2}}.$$

Then the ϕ integral is simply a convolution of two Gaussians and yields another Gaussian.

$$f_n(v) = \int d\Delta v \, \frac{1}{\sqrt{\pi}\,\frac{\sqrt{2}\,\Delta\phi}{mv}} e^{-\frac{(\Delta v)^2}{\left(\frac{\sqrt{2}\,\Delta\phi}{mv}\right)^2}} \cdot f_{n-1}(v - \Delta v), \tag{23}$$

where we have made the replacement $v = v_i - \Delta v$, and assumed $1/2\, mv^2 - 1/2\, mv_i^2 \approx mv\Delta v$. Thus, for velocities $v \gg \sqrt{2/m\,\Delta\phi}$, Eq. 23 has the form of a Kolmogorov equation, and we recover a diffusion equation. The diffusion constant is simply $\left(\frac{\sqrt{2}\,\Delta\phi}{mv}\right)^2$, and the Fokker-Planck equation[11] is

$$\frac{\partial f}{\partial n} = \frac{\partial}{\partial v}\left(\frac{\sqrt{2}\,\Delta\phi}{mv}\right)\frac{\partial f}{\partial v}. \tag{24}$$

Equation 24, if it were valid at low velocities, would predict a very large diffusion constant, infinite for $v = 0$. At low velocities, however, the maximum change in Δv^2 for one transit is given approximately by $1/m\,\Delta\phi$, the diffusion constant evaluated for v set equal to the "trapping width" $v = \sqrt{\frac{2\Delta\phi}{m}}$. Let us assume that even for trapped particles, the equation for $f(v, n)$ is still a diffusion equation:

$$\frac{\partial f}{\partial n} = \frac{\partial}{\partial v} D \frac{\partial f}{\partial v}. \tag{25}$$

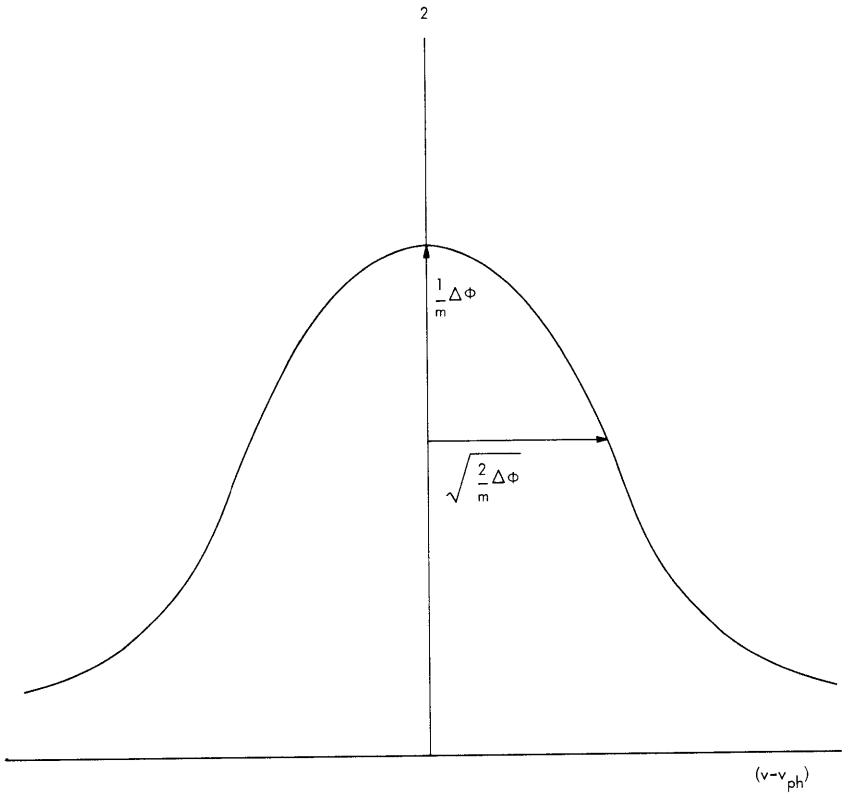

Fig. X-7. Plot of D(v).

Then D(v) is as shown in Fig. X-7. If an approximate analytic expression is desired for D(v), the formula

$$D(v) = \frac{\left(\frac{\sqrt{2}\,\Delta\phi}{m}\right)^2}{v^2 + \frac{2\Delta\phi}{m}}$$

will give the proper maximum at v = 0, the proper characteristic width, and the proper asymptotic behavior for large v. Let us recall that D is measured in the wave frame. Thus the curve is actually centered about the phase speed of the wave v_{ph}. Hence a particle can diffuse farther than the trapping width of the wave.

4. Discussion

We would like to examine the results of the computer experiments of Dawson,[6] and of Bers and Davis[7,8] in the light of the acceleration mechanism proposed here. Dawson's sets up a Maxwellian plasma (charge sheet model) at time t = 0, with thermal velocity v_T. This plasma coexists with a distribution of energetic electrons having thermal velocity v_T, and is centered at velocity 3.5 v_T; the classic "bump-on-tail"

situation.[1] He imposed periodic boundary conditions on the particle motion.

Dawson observed that the bump initially flattens in accordance with the predictions of quasi-linear theory. But the wave spectrum is not stationary as predicted, and it fluctuates rapidly in time. Also both the waves and particles are accelerated to high velocity. He associates the fluctuations in the wave spectrum with Cerenkov emission and absorption of waves. He also shows that waves may be scattered by particles to higher phase velocities.

The time scale on which the particles are accelerated to twice the initial beam velocity is roughly 6 to 8 transit times for the energetic particles. This suggests that another mechanism, which may also be important, is that the transit time effect diffuses the particles beyond the wave phase velocities. These particles then radiate high-velocity waves via Cerenkov emission. It seems likely that the observed effect is explained by a combination of these two mechanisms.

Bers and Davis set up a charge-sheet model of a beam-plasma system. They find that an electric field strong enough to trap the plasma electrons is set up at one point in space. A long time later, however, these trapped electrons have a distribution of velocities whose characteristic spread is considerably greater than the trapping width $(2\Delta\phi/m)^{1/2}$. Although it is difficult to observe directly, the wave spectrum appears to be largely between $0.6v_b < v_p < 0.8v_b$, where v_b is the original beam velocity, and v_p is the phase velocity of the wave. Under the assumption that half the beam energy goes into the production of these electrostatic waves, the trapping width is roughly $0.3v_b$ on each side of the phase velocity.

Bers and Davis observed trapped particles with all velocities from zero to twice the beam velocity. The fact that the distribution acquires this spread after approximately 10 transits suggests that transit-time diffusion may be an important contributing factor to the spread in velocity.

Let us remark, however, that as in Dawson's experiment, many other effects may come into play. For example, Bers and Davis do not use either periodic or perfectly reflecting boundary conditions. Instead, they use a time-variant electrostatic sheath to reflect the electrons back into the plasma. Thus there is a possibility that electrons may gain or lose energy on being reflected back into the system. Thus in each of these beam-plasma computer experiments, transit-time diffusion is probably important, but appears to be just one of several competing effects.

W. M. Manheimer

References

1. W. E. Drummond and D. Pines, Ann. Phys. (N.Y.) 28, 478 (1964).
2. T. H. Dupree, Phys. Fluids 9, 1773 (1966).
3. T. H. Stix, Phys. Fluids 7, 1960 (1964).

4. S. Puri, Phys. Fluids 9, 1043 (1966).

5. S. Puri, Phys. Fluids 9, 2043 (1966).

6. J. M. Dawson and R. Shanny, "Some Investigations of Nonlinear Behavior of One Dimensional Plasmas," Report Matt-568, Princeton University, Princeton, New Jersey, February 1968.

7. John Davis, Ph. D. Thesis, Department of Electrical Engineering, M. I. T., June 1967.

8. A. Bers and John Davis, Quarterly Progress Report No. 87, Research Laboratory of Electronics, M. I. T., October 15, 1967, p. 81.

9. W. B. Davenport, Jr., and W. L. Root, Introduction to the Theory of Random Signals and Noise (McGraw-Hill Book Company, New York, 1958), pp. 81-84.

10. T. S. Brown, Ph. D. Thesis, Department of Nuclear Engineering, M. I. T., February 1968.

11. Of course it is not clear from Eq. 23 that the Fokker-Planck equation has the form of a diffusion equation as shown, but only that $\frac{\langle \Delta v^2 \rangle}{\Delta n} = \left(\frac{\sqrt{2}\,\Delta\phi}{mv}\right)^2$. For the sake of convenience, we assume that a diffusion equation would follow from a more thorough analysis.